ACCEPTED VERSION

This is the accepted version of the following article:

which has been published in final form at http://dx.doi.org/10.1002/cmdc.202000280

Short Photoswitchable Antibacterial Peptides

Yuan Qi Yeoh,[a] John R. Horsley,*[a] Jingxian Yu,[a] Steven W. Polyak,[b,1] Blagojce Jovcevski[c] and Andrew D. Abell.*[a]

[a]   Y. Q. Yeoh, Dr. J. R. Horsley, Dr. J. Yu, Prof. A. D. Abell
        ARC Centre of Excellence for Nanoscale BioPhotonics (CNBP),
        Institute of Photonics and Advanced Sensing (IPAS),
        School of Physical Sciences,
        The University of Adelaide,
        North Terrace, Adelaide SA 5005, Australia.
        Email: andrew.abell@adelaide.edu.au
                john.horsley@adelaide.edu.au

[b]   Dr. S. W. Polyak
        School of Biological Sciences,
        Department of Molecular and Cellular Biology,
        The University of Adelaide,
        North Terrace, Adelaide SA 5005, Australia.

[c]   Dr. B. Jovcevski
        Adelaide Proteomics Centre,
        Department of Chemistry,
        School of Physical Sciences,
        The University of Adelaide,
        North Terrace, Adelaide SA 5005, Australia.

*Corresponding Authors

[1]   Present address: UniSA: Clinical and Health Sciences, University of South Australia, North Terrace, Adelaide, SA 5000, Australia.

Abstract

Three photoswitchable tetrapeptides, based on a known synthetic antibacterial, were designed and synthesized to determine activity against *Staphylococcus aureus* (*S. aureus*). Each peptide contains an azobenzene photoswitch incorporated into either the N-terminal side chain (**1**), C-terminal side chain (**2**), or the C-terminus (**3**), to allow reversible switching between *cis*- and *trans*-enriched photostationary states (PSS). Biological assays revealed the C-terminal azobenzene (**3**) possessed the most potent antibacterial activity, with an MIC of 1 µg/mL. In this study, net positive charge, hydrophobicity, position of the azobenzene, secondary structure, and amphiphilicity were all found to contribute to antibacterial activity, with each of these factors likely facilitating the peptide to disrupt the negatively charged bacterial lipid membrane. Hence, these short photoswitchable antibacterial tetrapeptides provide insights for the future design and synthesis of antibiotics targeting *S. aureus*.

Introduction

Photopharmacology is an emerging strategy to modulate the bioactivity of a compound using a reversible molecular switch (photoswitch) to provide localized treatment of an associated disease.[1] This approach offers an opportunity to mitigate off-target side effects,[1b, 2] and in the context of an antibiotic, the development of resistance.[1b] This typically involves incorporating a photoswitch, such as an azobenzene, into a compound, such as a peptide, to induce a change in physical and chemical properties upon photoisomerization with light of a specific wavelength.[3] The use of light in this context can be fine-tuned with high spatiotemporal precision,[1a, 4] allowing delivery of a bioactive compound. An azobenzene can be interconverted between *cis* and *trans* isomers on irradiation with UV and visible light respectively, resulting in a significant change in configuration and dipole moment.[5] Moreover, an azobenzene photoswitch provides a high photoisomerization yield, fast isomerization, low rate of photobleaching, and relative ease of synthesis.[4b, 6] We have previously reported photoswitching of an azobenzene-containing cyclic peptide based on a natural antibiotic, gramicidin S,[7] along with the use of an azobenzene to regulate biosensors,[8] protease inhibitors,[9] and smart membranes.[10] Herein, we present the design, synthesis and evaluation against *S. aureus* of three photoswitchable tetrapeptides (**1-3**, Figure 1). An azobenzene photoswitch was incorporated into either the side chain (peptides **1** and **2**) or the C-terminus

(peptide **3**) in order to explore the optimum position for photoswitching between *trans*- and *cis*-enriched PSS.

Results and Discussions

The design of peptides **1**-**3** (Figure 1) is based upon a known compound by Lau et al.,[11] (compound **23**, NH_2-BRBR-$CONH_2$, where B = *p*-phenyl-phenylalanine) which was reported to have antibacterial activity against methicillin-resistant *S. aureus* (MRSA, Minimal inhibitory concentration (MIC) 5 µg/ml).[11] Peptides **1** and **2** each contain a *p*-phenylazophenylalanine, azobenzene photoswitch which closely mimics the structure of the biphenyl side chains of compound **23**.[11] Specifically, the N-terminal biphenyl of compound **23**[11] was replaced with an azobenzene photoswitch in peptide **1**, while the C-terminal biphenyl was replaced with an azobenzene in peptide **2**. Peptide **3** has the same azobenzene photoswitch directly attached to the C-terminus. The rational positioning of the azobenzene photoswitch into each of peptides **1**-**3** allows retention of the overall positive charge (+3) in each case. The free amines located at the N-terminus and both side chains of each arginine residue remain available for protonation, and are crucial for antibacterial activity of compound **23** and other peptides targeting Gram-positive bacteria [11-12] through establishment of electrostatic interactions for binding to the negatively charged bacterial membrane.[13] The design of peptides **1**-**3** exploits the knowledge that the azobenzene photoswitch induces a change in dipole moment upon photoisomerization,[5, 14] which in turn affects the amphiphilicity[15] that is crucial to antibacterial activity.[7, 16] Each peptide was synthesized using standard Fmoc solid phase peptide synthesis (SPPS) and purified by RP-HPLC, as outlined in the Supporting Information. The component azobenzene photoswitch was synthesized using an existing methodology.[9a]
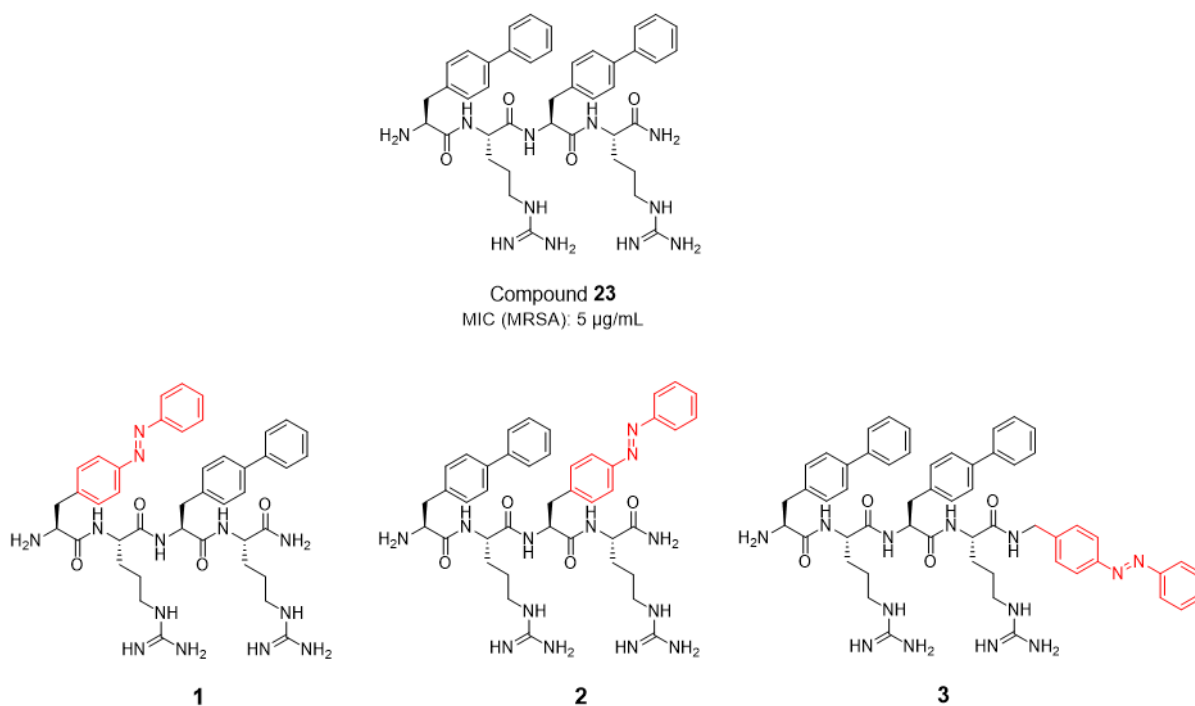
Compound **23**
MIC (MRSA): 5 μg/mL

1   **2**   **3**

Figure 1. Chemical structures for compound **23**[11] and peptide mimetics **1**-**3** (*trans* conformations are shown). The azobenzene photoswitch is highlighted in red.

Samples of peptides **1**-**3** were separately irradiated with visible light (405 nm) for 2h to yield the associated *trans*-enriched PSS, and the UV-Vis absorbance for each was reported (Figure S4). The *trans*-enriched PSS for each of peptides **1**-**3** showed an intense absorption band, with a maximum absorbance at 328 nm due to the symmetry-allowed π→π* transition. Each peptide was then exposed to UV light (352 nm) for 2h to give the associated *cis*-enriched PSS, and the absorbance spectra reported (Figure S4). The *cis*-enriched PSS for each of peptides **1**-**3** exhibited a weak absorption at 428 nm resulting from the forbidden n→π* transition, with a significantly reduced absorption at 328 nm. These absorbance values concur with literature, where both isomers of the azobenzene are known to give distinct but slightly overlapping absorption spectra.[4a, 17]

The maximum photoisomerization yield of peptides **1**-**3** was determined by ^{1}H NMR analysis, particularly comparison of resonances corresponding to the *para*-substituted phenyl ring in the azobenzene photoswitch.[7] Specifically, the resonances at δ 7.85 ppm and δ 6.78 ppm for peptide **1**, δ 7.81 ppm and δ 6.74 ppm for peptide **2**, and δ 7.85 ppm and δ 6.76 ppm for peptide **3** were

used to calculate these ratios (Figures S11-S13). Relatively high photoisomerization yields for each PSS were observed, with *trans*-enriched PSS of 100%, 88% and 85%, and *cis*-enriched PSS of 86%, 86%, and 91% for peptides **1**-**3** respectively (Table 1). Detailed ^{1}H NMR spectroscopy also confirmed the structural conformation of each peptide. Interestingly, $^3J_{\text{NH-C}\alpha\text{H}}$ coupling constants between 7.5-10 Hz[18] were observed for both *cis*- and *trans*-enriched PSS of peptides **1**-**3**, indicating the presence of a β-strand geometry for each (Table S2). To further define secondary structure, the *cis* and *trans* isomers of peptides **1**-**3** were analyzed by density functional theory (DFT). Calculated dihedral angles for both *cis* and *trans* isomers of peptides **1**-**3** were consistent with a β-strand conformation[19] (Table S1, Figure S7), in line with the ^{1}H NMR data. Collectively, these findings indicate that the incorporation of an azobenzene photoswitch into either the side chain or the C-terminus of the peptides does not result in a significant change in secondary structure upon photoisomerization. Thus, any differences in antibacterial activity are likely attributable to other factors, such as the azobenzene position and amphiphilicity, and these are discussed later.

Half-lives for the *cis*-enriched PSS of each peptide were determined by measuring the kinetics of *cis-trans* thermal back isomerization, as detailed in the Supporting Information. Briefly, samples of peptides **1**-**3** were each irradiated under UV light (352 nm) for 2.5h to provide the maximum attainable *cis*-enriched PSS. Each peptide in its *cis*-enriched PSS was then stored in the dark to switch to the respective *trans*-enriched PSS by thermal relaxation. The absorbance for each was measured every 10 min to monitor the change in absorbance at 328 nm, which is characteristic of the *trans*-enriched PSS. The half-life for each peptide was then calculated by extrapolating the curve, and the data analyzed using GraphPad Prism 8 software.[20] The *cis*-enriched PSS for each of peptides **1**-**3** possess comparable half-lives of 43.4h, 44.6h and 40.8h respectively, thus affording sufficient time for antibacterial assaying against *S. aureus* (24h).

Table 1. Photoisomerization yields and half-lives of peptide mimetics **1-3**, in their respective photostationary states (PSS).

Peptide	Photoisomerization yield (%)		Half-life for *cis*-enriched PSS (h)
	trans-enriched PSS	*cis*-enriched PSS	
1	100	86	43.4
2	88	86	44.6
3	85	91	40.8

The two photostationary states of peptides **1-3** were assayed against *S. aureus* ATCC 49775 (see Supporting Information), as model compound **23**[11] is active against this bacterial species. Each peptide was dissolved in DMSO at a concentration of 8 mg/mL, and irradiated separately using either UV (352 nm) or Vis (405 nm) light for 2h to obtain the respective *cis*- and *trans*-enriched PSS, which were then subjected to antimicrobial susceptibility assays.[21] Peptide **1**, containing an azobenzene moiety to mimic the N-terminal biphenyl side chain of synthetic tetrapeptide (compound **23**[11]), displayed a modest antibacterial activity with MICs of 16 µg/mL and 64 µg/mL for the *trans*- and *cis*-enriched PSS respectively (Table 2). Replacement of the C-terminal biphenyl side chain moiety with an azobenzene photoswitch, as in peptide **2**, increased antibacterial activity with MICs of 8 µg/mL and 32 µg/mL for the *trans*- and *cis*-enriched PSS, respectively. As peptides **1** and **2** both possess an identical amino acid composition and similar secondary structure, these disparate antibacterial properties likely reflect the influence of the position of the azobenzene photoswitch. However, a four-fold difference in the MIC values between the *cis*- and *trans*-enriched PSS of peptides **1** and **2** was observed (Table 2), suggesting that in addition to the specific location of the azobenzene moiety, the intrinsic properties of the photoswitch contribute to antibacterial activity. This four-fold disparity is likely due to a change in overall amphiphilicity,[7] as the azobenzene photoswitch induces a considerable change in the dipole moment upon photoisomerization.[5] As the *trans*-enriched PSS of peptides **1** and **2** most closely resemble the structure of the synthetic tetrapeptide (compound **23**[11]), it was not surprising that these were more active in suppressing growth of *S. aureus* than their *cis*-enriched counterparts. Notably, the *trans*-enriched PSS of peptide **3** exhibited far superior antibacterial activity over peptides **1** and **2**, with a particularly potent MIC of 1 µg/mL against *S. aureus*, again demonstrating the significance of the position of the azobenzene photoswitch. The *cis*-enriched PSS of peptide **3** was found to be

insoluble in the assay medium, which further supports a change in hydrophobicity and overall amphiphilicity upon photoisomerization. Furthermore, the additional aromatic groups in peptide **3** increased the hydrophobicity of the compound in comparison to peptides **1** and **2**, as evidenced by the longer retention time observed by RP-HPLC (Figure S3). Placement of the azobenzene photoswitch at the C-terminus of peptide **3** provides increased hydrophobicity without altering the net positive charge, thus affording optimum amphiphilicity. These properties are clearly advantageous for the designed peptide to disrupt the bacterial lipid membrane, thereby providing a practical insight into the possible mechanism for antibacterial activity.

Table 2. Minimum inhibitory concentration (MIC) for the *trans*-enriched and *cis*-enriched PSS of peptide mimetics **1**-**3** against *S. aureus* ATCC 49775. The MIC for the *cis*-enriched PSS of peptide **3** was not determined due to its insolubility in the assay medium. (* ND – not determined)

Peptide mimetics	Minimum Inhibitory Concentration, MIC (µg/mL)	
	trans-enriched PSS	*cis-enriched* PSS
1	16	64
2	8	32
3	1	ND*

In summary, three short photoswitchable antibacterial peptides, based on a known synthetic tetrapeptide, were designed and synthesized to investigate antibacterial activity against *S. aureus*. Each peptide (**1**-**3**) contains an azobenzene photoswitch incorporated either on a side chain (**1-2**) or the C-terminus (**3**), to allow reversible switching between the *cis*- and *trans*-enriched PSS. Biological testing against *S. aureus* revealed a four-fold difference in the antibacterial activity between the *cis*- and *trans*-enriched PSS of peptides **1** and **2**, revealing a change in overall amphiphilicity brought about by a change in dipole moment upon photoisomerization. A two-fold difference in the antibacterial activity between peptides **1** and **2** was also observed, and attributed to the positioning of the azobenzene photoswitch, as both peptides contain an identical amino acid composition and similar secondary structure as defined by the earlier ^{1}H NMR analysis and modelling. In each case, the *trans*-enriched PSS was more potent than its *cis*-enriched counterpart, as it most closely mimics the structure of the biphenyl side chain of the known antibacterial. The *trans*-enriched PSS of peptide **3** exhibited the most potent antibacterial activity, with an MIC of 1

μg/mL against *S. aureus*. The position of the azobenzene photoswitch is also conspicuous in **3**, as it allows an increase in hydrophobicity within the peptide without disrupting the net positive charge. Hydrophobicity and an overall positive charge are clearly desirable properties to enable the peptide to disrupt the negatively charged bacterial lipid membrane of *S. aureus*. Furthermore, as each *cis-* and *trans*-enriched PSS for each peptide was found to contain a β-strand geometry, it is likely that this well-defined secondary structure provides the fundamental framework to stabilize the amino acid residues responsible for maintaining amphiphilicity. Hence, an overall positive charge, hydrophobicity, azobenzene position and amphiphilicity were all found to be crucial in promoting antibacterial activity.

Acknowledgements

References

[1]   a) K. Hüll, J. Morstein, D. Trauner, *Chem. Rev.* **2018**, *118*(21), 10710–10747; b) W. A. Velema, W. Szymanski, B. L. Feringa, *J. Am. Chem. Soc.* **2014**, *136*(6), 2178–2191.

[2]   a) M. M. Lerch, M. J. Hansen, G. M. van Dam, W. Szymanski, B. L. Feringa, *Angew. Chemie Int. Ed.* **2016**, *55*(37), 10978–10999; b) M. Wegener, M. J. Hansen, A. J. M. Driessen, W. Szymanski, B. L. Feringa, *J. Am. Chem. Soc.* **2017**, *139*(49), 17979–17986.

[3]   M. Feliciano, D. Vytla, K. A. Medeiros, J. J. Chambers, *Bioorg. Med. Chem.* **2010**, *18*(22), 7731–7738.

[4]   a) A. A. Beharry, G. A. Woolley, *Chem. Soc. Rev.* **2011**, *40*(8), 4422–4437; b) W. Szymański, J. M. Beierle, H. A. V. Kistemaker, W. A. Velema, B. L. Feringa, *Chem. Rev.* **2013**, *113*(8), 6114–6178.

[5]   a) H. Fliegl, A. Köhn, C. Hättig, R. Ahlrichs, *J. Am. Chem. Soc.* **2003**, *125*(32), 9821–9827; b) E. Merino, M. Ribagorda, *Beilstein J. Org. Chem.* **2012**, *8*, 1071–1090.

[6]   a) A. S. Lubbe, W. Szymanski, B. L. Feringa, *Chem. Soc. Rev.* **2017**, *46*(4), 1052–1079; b) Z. Mahimwalla, K. G. Yager, J.-i. Mamiya, A. Shishido, A. Priimagi, C. J. Barrett, *Polym. Bull.* **2012**, *69*(8), 967–1006; c) M. S. Maier, K. Hüll, M. Reynders, B. S. Matsuura, P. Leippe, T. Ko, L. Schäffer, D. Trauner, *J. Am. Chem. Soc.* **2019**, *141*(43), 17295–17304.

[7]   Y. Q. Yeoh, J. Yu, S. W. Polyak, J. R. Horsley, A. D. Abell, *ChemBioChem* **2018**, *19*(24), 2591–2597.

[8]   J. R. Horsley, J. Yu, K. L. Wegener, C. Hoppmann, K. Rück-Braun, A. D. Abell, *Biosens. Bioelectron.* **2018**, *118*, 188–194.

[9]   a) B. Blanco, K. A. Palasis, A. Adwal, D. F. Callen, A. D. Abell, *Bioorg. Med. Chem.* **2017**, *25*(19), 5050–5054; b) D. Pearson, A. D. Abell, *Chem. Eur. J.* **2010**, *16*(23), 6983–6992.

[10]   T. Kumeria, J. Yu, M. Alsawat, M. D. Kurkuri, A. Santos, A. D. Abell, D. Losic, *Adv. Mater.* **2015**, *27*(19), 3019–3024.

[11]   Q. Y. Lau, F. M. Ng, J. W. D. Cheong, Y. Y. A. Yap, Y. Y. F. Tan, R. Jureen, J. Hill, C. S. B. Chia, *Eur. J. Med. Chem.* **2015**, *105*, 138–144.

[12]   Y. Q. Yeoh, J. R. Horsley, S. W. Polyak, A. D. Abell, *Bioorg. Med. Chem. Lett.* **2020**, *30*(11), 127140.

[13]   a) J. P. Bradshaw, *BioDrugs* **2003**, *17*(4), 233–240; b) E. M. Kohn, D. J. Shirley, L. Arotsky, A. M. Picciano, Z. Ridgway, M. W. Urban, B. R. Carone, G. A. Caputo, *Molecules (Basel, Switzerland)* **2018**, *23*(2), 329; c) J. A. Tennessen, *J. Evol. Biol.* **2005**, *18*(6), 1387–1394.

[14]   E. Wagner-Wysiecka, N. Łukasik, J. F. Biernat, E. Luboch, *J. Incl. Phenom. Macro.* **2018**, *90*(3), 189–257.

[15]   a) D. Eisenberg, R. M. Weiss, T. C. Terwilliger, W. Wilcox, *Faraday Symp. Chem. Soc.* **1982**, *17*, 109–120; b) J. Y. Park, M. Umashankar, D. S. Huh, *Macromol. Res.* **2016**, *24*(4), 350–358.

[16]   O. Babii, S. Afonin, M. Berditsch, S. Reiβer, P. K. Mykhailiuk, V. S. Kubyshkin, T. Steinbrecher, A. S. Ulrich, I. V. Komarov, *Angew. Chemie Int. Ed.* **2014**, *53*(13), 3392–3395.

[17]   a) L. Albert, O. Vázquez, *ChemComm* **2019**, *55*(69), 10192–10213; b) H. M. D. Bandara, S. C. Burdette, *Chem. Soc. Rev.* **2012**, *41*(5), 1809–1825.

[18]   S. R. L. Fernando, G. V. Kozlov, M. Y. Ogawa, *Inorg. Chem.* **1998**, *37*(8), 1900–1905.

[19]   A. D. Abell, N. A. Alexander, S. G. Aitken, H. Chen, J. M. Coxon, M. A. Jones, S. B. McNabb, A. Muscroft-Taylor, *J. Org. Chem.* **2009**, *74*(11), 4354–4356.

[20]   A. Desponds, R. Freitag, *Langmuir* **2003**, *19*(15), 6261–6270.

[21]   K. J. Lee, W. Tieu, B. Blanco-Rodriguez, A. S. Paparella, J. Yu, A. Hayes, J. Feng, A. C. Marshall, B. Noll, R. Milne, D. Cini, M. C. J. Wilce, G. W. Booker, J. B. Bruning, S. W. Polyak, A. D. Abell, *ACS Chem. Biol.* **2019**, *14*(9), 1990–1997.